REVIEW ARTICLE

How chromosome topologies get their shape: views from proximity ligation and microscopy methods

Yike Huang, Roel Neijts (iD) and Wouter de Laat (iD)

Oncode Institute, Hubrecht Institute-KNAW, University Medical Center Utrecht, Utrecht, the Netherlands

Correspondence

W. de Laat, Oncode Institute, Hubrecht Institute-KNAW and University Medical Center Utrecht, Uppsalalaan 8,3584 CT Utrecht, the Netherlands
Tel: +31 30 212 1800
E-mail: w.laat@hubrecht.eu

Yike Huang and Roel Neijts have equal contribution

Edited by Claus Azzalin

The 3D organization of our genome is an important determinant for the transcriptional output of a gene in (patho)physiological contexts. The spatial organization of linear chromosomes within nucleus is dominantly inferred using two distinct approaches, chromosome conformation capture (3C) and DNA fluorescent *in situ* hybridization (DNA–FISH). While 3C and its derivatives score genomic interaction frequencies based on proximity ligation events, DNA–FISH methods measure physical distances between genomic loci. Despite these approaches probe different characteristics of chromosomal topologies, they provide a coherent picture of how chromosomes are organized in higher-order structures encompassing chromosome territories, compartments, and topologically associating domains. Yet, at the finer topological level of promoter–enhancer communication, the imaging-centered and the 3C methods give more divergent and sometimes seemingly paradoxical results. Here, we compare and contrast observations made applying visual DNA–FISH and molecular 3C approaches. We emphasize that the 3C approach, due to its inherently competitive ligation step, measures only 'relative' proximities. A 3C interaction enriched between loci, therefore does not necessarily translates into a decrease in absolute spatial distance. Hence, we advocate caution when modeling chromosome conformations.

Keywords: chromosome conformation capture; DNA fluorescent *in situ* hybridization; live-cell imaging; gene regulation; genome organization; loop extrusion; promoter–enhancer interaction

How the linear chromatin fiber is 3D folded within the nuclear space and how these conformational states are related to gene expression in healthy and pathological conditions have gained major attention over the past decades. DNA–fluorescent *in situ* hybridization (DNA–FISH) and chromosome conformation capture (3C)-based approaches have been mainstream in pushing forward our knowledge of the functional 3D organization of chromosomal fibers. These two complementary methodologies can capture the distribution of conformational possibilities in a population of cells at a defined time point, when conformational states become cross-linked. Yet, DNA–FISH and 3C methodologies are distinct in their setup, in the experimental biases and in the information that they provide on chromosomal conformations.

DNA–FISH comes in various flavors and, in short, enables the visualization of genomic loci within their nuclear volume by means of fluorescently labeled probes that specifically hybridize with and thereby tag

Abbreviations

3C, chromosome conformation capture; CT, chromosome territory; CTCF, CCCTC-binding factor; DamID, DNA adenine methyltransferase identification; DNA–FISH, DNA–fluorescent *in situ* hybridization; ESC, embryonic stem cell; LAD, lamina-associated domain; LCR, locus control region; SCR, *Sox2* control region; TAD, topologically associating domain.

a given region of interest [1]. Recent innovations such as Oligopaint permit consecutive labeling of large genomic intervals with fluorescent probes, making visualization no longer restricted to only a small number of loci [2]. Besides measuring physical distances between genomic segments, DNA–FISH traces their radial positions within the nuclear volume and the compactness of a given locus in transcriptionally active or inactive states can be measured [3–6].

DNA-FISH is an image-centered approach and greatly differs from 3C-based genomic mapping methodologies, in which cross-linked chromatin fibers are subjected to digestion and subsequent ligation, ultimately to score how often certain genomic fragments are ligated to fragments that are in spatial proximity [7]. Similar to DNA–FISH, 3C-based approaches can be applied to study either a single locus or larger regions, or even the entire genome. As a method that is inherently powerful at cell population level, either by bulk or on cumulative single-cell analysis, 3C-based technologies have made major contributions to the definition of topological metastructures such as A/B compartments, topologically associating domains (TADs), and smaller intra-TAD structures [8–13]. In contrast to DNA–FISH, 3C-based analysis cannot inform on the intranuclear position of a given locus.

In this review, we focus on the topological features and concepts that have emerged from the use of DNA–FISH and 3C technologies. We discuss that there is a strong consensus between DNA–FISH- and 3C-based observations on large-scale genomic conformations. However, concerning the conformations states below the level of TADs, some recent results obtained by the respective approaches intuitively seem to reach divergent conclusions. These contrasting observations touch upon a long-standing question: Is spatial proximity between promoter and enhancer a prerequisite for gene expression?

Intranuclear consensus by DNA–FISH and 3C approaches

The spatial distribution of linear chromatin fibers inside the nuclear volume is not random but is structurally organized at various topological levels. Recognizable chromatin structures include, from the largest to the smallest, chromosome territories (CTs), A/B compartments, TADs, and intra-TAD structures including enhancer–promoter loops and polycomb-repressive bundles contacts [12]. With regard to higher-order levels of organization, that is, the CTs, A/B compartments, and TADs, DNA fluorescent labeling and 3C-based methods concur on both their existence and nature (Fig. 1).

Level 1: Chromosome territories

The largest higher-order conformation, the CT, was initially hinted upon in the late 19th century by light microscopy [14,15]. Almost a century later, different chromosome labeling techniques including DNA–FISH confirmed that individual chromosomes are not intermingled in nuclear space, but are confined to spatial domains thereby highly, but not exclusively, self-interacting [16] (Fig. 1). By the sole use of the molecular 3C approach, the existence of CTs can be reconstituted as well. For instance, the vast majority of interaction partners for a given 4C genomic viewpoint fragment is always mapped to the same chromosome [17]. Experiments from the earliest days of population and single-cell Hi-C demonstrated similar contact distributions within and between chromosomes [8,18]. Preferred chromosome self-interactions translate into the distinct chromosomal interaction blocks that are seen in Hi-C genomic contact matrices, representing the ligation-based equivalents to the CTs that were initially visualized by microscopy in the nuclear volume (Fig. 1). In diploid nuclei, DNA–FISH allows observing the two homologous chromosomes and finds them occupying distinct territories. In line with this notion, Hi-C performed on murine hybrid cells that carry two subspecies-specific alleles reveals that the individual homologs of a chromosome pair form their own interaction blocks [19]: They contact each other as frequently as any of the other chromosomes. Thus, both 3C-based and DNA labeling approaches show that individual chromosomes self-aggregate in CTs that only allow limited interchromosomal intermingling.

Level 2: A/B compartments

One topological step lower, 3C and DNA–FISH findings share further consensus. Locus-specific DNA–FISH demonstrated that transcribed or silent genes colocalize in their respective active and inactive nuclear compartments [20]. This separation of active and inactive loci could be recapitulated by proximity ligation approaches as well. 4C demonstrated that the collection of *cis*-contacts of the β-globin locus highly differs between transcriptional states [17]. In β-globin-silent tissues, the locus is contacting other regions with non-expressed genes elsewhere on the same chromosome fiber, whereas in fetal liver cells the transcriptionally active locus predominantly interacts with active *in cis* regions Generally, inactive and active hubs could
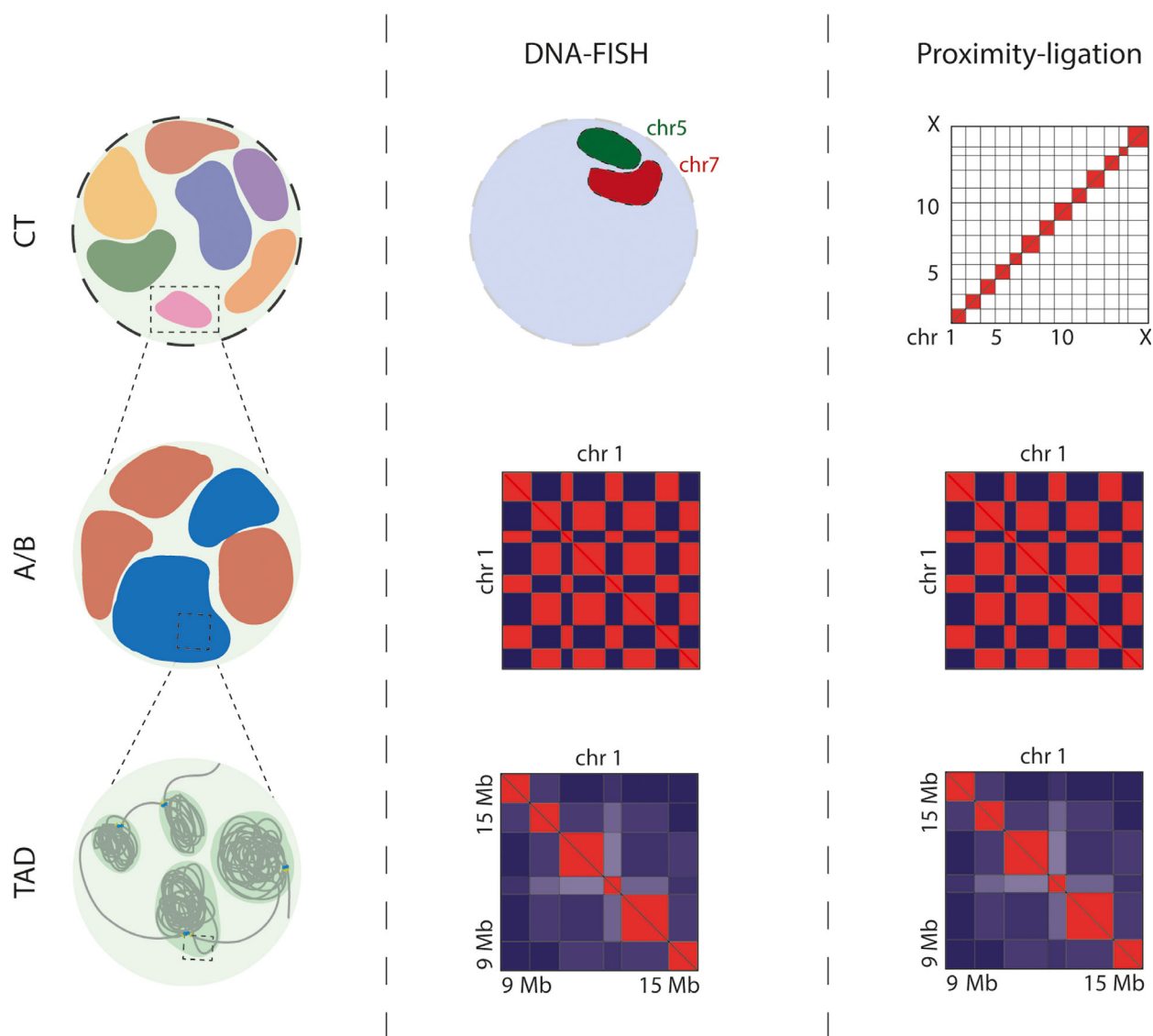
Fig. 1. Consensus on large-scale topologies observed by DNA–FISH and 3C. Left*:* Schematic overview of the 3D structures in which linear chromosome fibers are folded within the nucleus (dashed-line circle), from largest to smallest: CTs, A/B compartments (A/B), and TADs. Middle: Schematic representation on how these structures are observed by DNA–FISH. Right: Schematic representation on how these structures are observed by 3C-based methods. Individual chromosomes in CTs are observed by DNA–FISH as discrete intranuclear domains (green and red, representing chromosomes 5 and 7, respectively) and by 3C as squares representing the high degree of self-interaction of individual chromosomes. A checkerboard pattern, typical for A/B compartmentalization, schematically depicted for chromosome 1, becomes visual by both respective techniques. Finally, TADs are discernable as triangles along a chromosomal interval, by both DNA–FISH and proximity ligation approaches. See text for further details.

systematically be identified by using the genome-wide Hi-C approach and were referred to as active 'A' and inactive 'B' compartments [8,21] (Fig. 1). In whole-chromosome Hi-C matrices, compartments become apparent by their typical checkerboard-like distribution of interaction (Fig. 1). DNA–FISH analyses on selected single loci confirmed that sequences in the inactive B compartment are more frequently proximal

to linearly distant inactive loci, than to linearly nearby but active loci [8].

Until recently, DNA–FISH could only demonstrate the differential localization for a limited number of selected loci rather than providing an unbiased catalogue of spatial relationships between many individual loci on a chromosomal fiber. With the advent of Oligopaint, which allows walking along a large linear

chromosomal interval, DNA–FISH demonstrated to be a powerful tool to investigate spatial relationships in a systematic manner [2]. Combining the data on spatial distributions from many *cis*-alleles, Oligopaint-generated matrices are strikingly reminiscent to the contact maps obtained by Hi-C, including the characteristic checkerboard patterns of chromosomal compartmentalization [22,23] (Fig. 1).

Compartments become intensely rearranged during cellular differentiation and reprogramming [24–29]. For instance, as demonstrated by Hi-C, along the *in vitro* differentiation path from human embryonic stem cell (ESC) to cardiomyocyte, nearly one-fifth of the genome switches from the one compartment to the other [24]. Comparison between multiple human ESC-derived lineages shows that, in total, an approximate one-third of the genome can be subjected to A/B compartment switching during cellular differentiation [25]. Spatial compartmentalization thereby seems to be dictated by the trans-acting factors associated with the loci: artificial recruitment of either a pluripotency factor, a Polycomb group protein, or a constitutive heterochromatin factor directs a locus in ESCs to an active compartment with pluripotency genes, to a compartment enriched for Polycomb-controlled genes, or to an inactive compartment, respectively [30]. The switching behavior of genomic sequences from one compartment to another is also reported by imaging-based approaches. For instance, it has been demonstrated that the initial spatial colocalization of inactive loci and regions that become activated during B-cell maturation is no longer maintained upon differentiation. Concomitantly, activated regions move away from the nuclear periphery toward the nuclear interior [31].

As mentioned, the spatial repositioning in the nuclear volume of genomic loci cannot be recorded by the 3C toolbox. However, orthogonal molecular tools including DNA adenine methyltransferase identification (DamID), tyramide signal amplification, followed by sequencing (TSA-seq), and chromatin immunoprecipitation followed by sequencing (ChIP-seq) are able to partially complement 3C. For example, DamID-derived lamina-associated domains (LADs) are highly correlated with B compartments, providing Hi-C data a spatial dimension, albeit indirectly [32]. Combining Hi-C data with the recently developed GPSeq confirmed that A and B compartments are generally located more centrally and toward the nuclear periphery, respectively [33].

Together, the spatial segregation of active and inactive regions as probed by DNA–FISH, and the contact frequency patterns observed by 3C-based methods, concordantly describe the same higher-order rearrangements of structures referred to as A and B compartments.

Level 3: Topologically associating domains

Whereas A/B compartments represent large chromosomal fractions that are characterized by their interactional and epigenetic states, TADs form self-interacting domains within compartments, dominantly defined by their boundaries which are enriched of CCCTC-binding factor (CTCF) proteins [10]. TADs are considered as genomic segments in which *cis*-regulatory landscapes are canalized, as demonstrated by numerous genome-engineering experiments [34–38]. On a population-wide level, a large measure of agreement on the structural features of TADs is reached between 3C and DNA–FISH analysis. At the level of single cells, the two respective methodologies provide complementary insights of TAD organization.

The golden standard to define a TAD is provided by the 3C technology, which also stands at the root of its initial description [9–11]. TADs are visualized by 3C methods as triangular shapes along a chromosomal interval in contact matrices (Fig. 1). They can be detected when Hi-C or 5C is applied to populations of cells, in which case they represent average structures appreciable from superimposing sparse contact data collected from large numbers of individual alleles. Indeed, TADs are difficult to grasp from single-cell Hi-C datasets, but become visible when data of many individual cells are aggregated [18].

Currently, TADs are predominantly considered to arise from the dynamic interplay between the cohesin complex and the boundary protein CTCF. In the widely adopted mechanistic loop-extrusion model [39–41], the ring-shaped cohesin protein complex is loaded on chromosomal positions and generates loops as the chromatin fiber is progressively sliding through its ring. CTCF-bound sequences thereby function as boundary elements inhibiting the progression of cohesin, resulting in a relatively stable loop between convergent oriented CTCF binding sites [42–44]. Important clues in favor of the model originate from cellular depletions of the main components of the loop-extrusion model, that is, CTCF and members of the cohesin complex. Conditional depletion of CTCF followed by bulk Hi-C analysis demonstrated that the shaping of interphase chromosomes into TADs is highly affected. Loops are still being produced by cohesin, but they are no longer halted at the defined boundaries [45]. On cohesin-depleted chromosomes however, loops are no longer being extruded and

distant *cis*-elements are less likely to interact with their putative targets [46,47].

Additionally, Hi-C matrices from synchronized cell populations give insightful glimpses of the underlying dynamics that contribute to the formation of TADs. In cells that are immediately harvested after mitotic exit, certain individual genomic regions progressively interact with a continuum of genomic regions. This directional progression is captured over different sampled time points and can be reconstructed as a 'growing' stripe at CTCF-enriched borders in the Hi-C matrices [48], reminiscent to prediction by the loop-extrusion model.

DNA-FISH derative Oligopaint is uniquely qualified to analyze the detailed topology of individual alleles. By the consecutive hybridization steps along a genomic interval, it allows visualization and measurement of spatial distances between all labeled regions from the single linear molecule. Consequently, the reconstruction of the spatial morphology of an individual chromatin fiber is possible, for instance, for an interval that would encompass a TAD. In agreement with Hi-C findings, the Oligopaint strategy is able to recapitulate TADs when collapsing the observed structures of many individual alleles [22]. The profiles that arise from this spatial distribution mimic the proximity ligation-based triangular TAD structures as observed in Hi-C matrices (Fig. 1).

Single-cell analyses from the two respective approaches both demonstrate a high cell-to-cell heterogeneity in genome conformation. Single-cell Hi-C applied to numerous individual cells shows a rich collection in interaction partners for a given genomic fragment [18,49–51], whereas Oligopaint demonstrates a high heterogeneity in individual chromosomal conformations [23,52]. The spatial structures of linear fibers, visualized by Oligopaint and referred to as 'TAD-like structures', possess boundaries which positions vary from cell-to-cell, although they preferentially reside at CTCF-enriched positions [23]. From a single-cell perspective, TAD borders are thus rather flexible instead of physically absolute [23,53]. It is important to emphasize that TADs — originally identified and defined by 3C on population level — and TAD-like structures — based on single-cell Oligopaint reconstructions — are far from interchangeable definitions: they represent very different entities based on their respective statistical and physical nature [54].

Given the observation that TAD borders show already high variability between individual alleles, how would single chromosome fibers be impacted by the depletion of CTCF or Cohesin? Conditional degradation of the two main players of the loop-extrusion model, that is, CTCF and cohesin, followed by Oligopaint analyses confirms that they dominantly contribute to formation of TADs. On individual chromosomes, it was demonstrated that CTCF depletion leads to an increased spatial overlap between intervals that would normally be separated [53]. Contrary, removal of cohesin leads to decreased contacts within domains and between separated domains, suggesting that TAD boundaries may not be inherently absolute [53]. However, certain TAD structures were still present in cohesin-depleted cells [23], indicating that some compact conformations are not solely dependent on the presence of the loop extruder. These unaffected structures may include micro-TADs, polycomb-enriched domains, or as suggested by recent Micro-C studies, promoter–enhancer interactions that exist independently of loop extrusion [12,13].

In summary, concerning the cell population-based definition of TADs, findings by DNA–FISH and 3C-based results are highly compatible (Fig. 1). However, from a single-allele perspective, self-interacting domains can be interpreted differently from imaging and ligation-based approaches. For instance, the TAD-like entities as defined by Oligopaint are not detectable by 3C methodology in a same individual cell.

Intra-TAD paradox between labeling and proximity ligation assays

Whereas the independent findings of 3C and DNA–FISH methodologies on large-scale chromosomal organizations share many agreements, the two respective techniques may present different and seemingly paradoxical configurations at the level that immediately concerns gene regulation by *cis*-regulatory elements. In particular, recent imaging-based studies challenge the prevalent notion that enhancers and promoters require to get in close spatial proximity for transcriptional activation, while 3C-based experiments appear to support the concept of communication through proximity.

Probing proximity

One of the, if not the most, rudimentary observations uncovered by 3C approaches is the profound difference in enhancer–promoter contacts between transcriptional states of a locus (Fig. 2). For instance, the aforementioned murine β-globin locus adopts distinctive conformations in expressing and nonexpressing cells. Whereas in expressing blood cells, the active *Hbb-b1* gene gains more proximity ligation-based contacts with the *Locus Control Region* (*LCR*), the
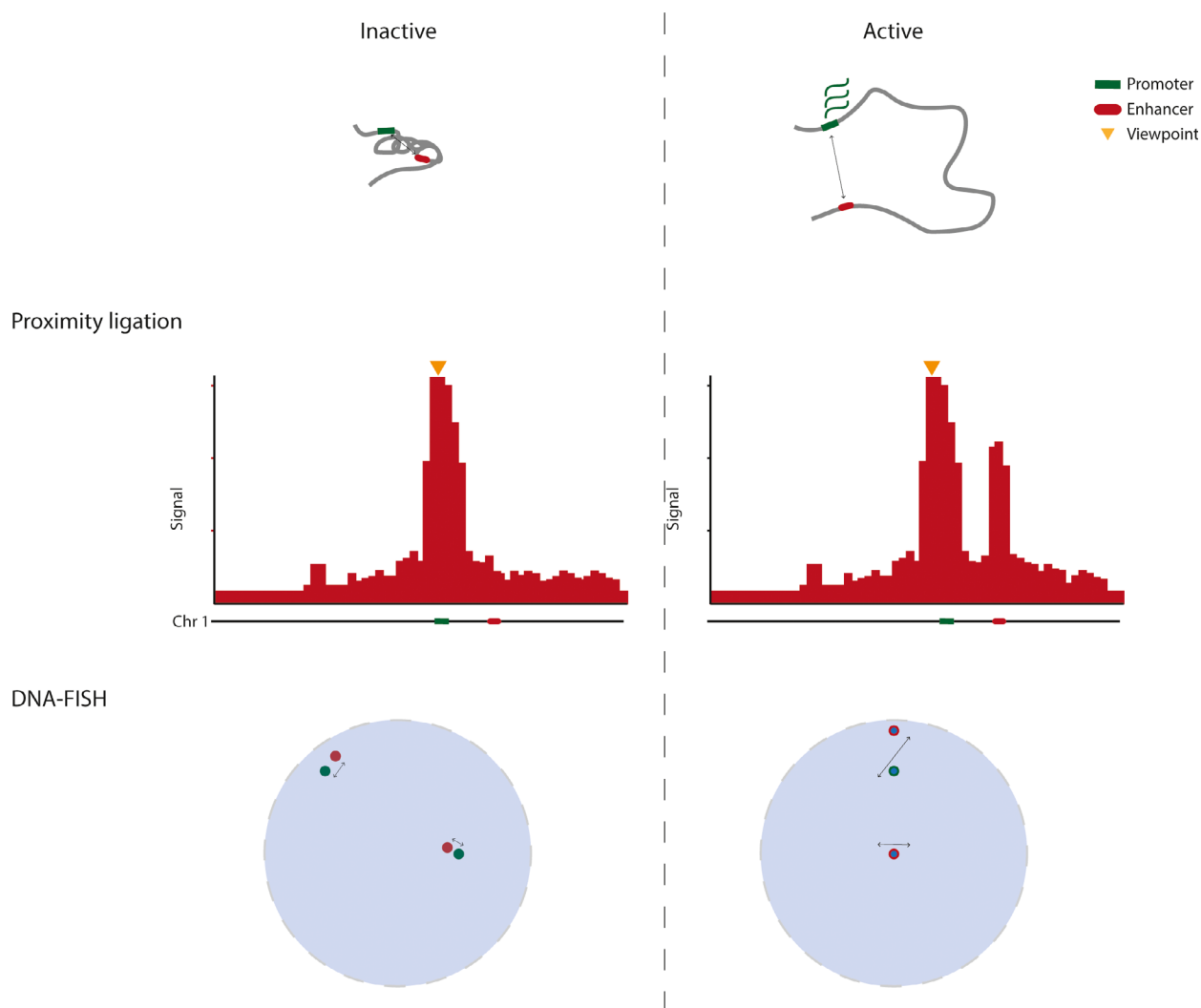
Fig. 2. Topological observations: spatial distance by DNA–FISH versus relative proximity ligation by 3C. Left*:* A hypothetical locus containing a gene promoter (green) and its enhancer (red) in an inactive, compacted state, and how this conformation is observed by 4C-seq seen from the promoter (viewpoint, yellow arrow), and by DNA–FISH. Right*:* The same locus, now active and decompacted, and how 4C-seq and DNA–FISH detect this conformation. Typically, upon transcriptional activation a gain of specific interaction between enhancer and promoter is observed by 4C-seq (enriched interaction with the enhancer, in red). This does not translate into a decrease in spatial distance between the activated enhancer and promoter, but rather leads to an increased distance as seen by DNA–FISH. Due to decompaction, the competition with other potential ligation partners in the 3C assay is reduced resulting in a relative gain of promoter–enhancer interaction as scored in the active conformation. Arrows indicate physical distances between enhancer and promoter. See text for further details.

superenhancer essential for high expression level of all β-globin genes, the locus remains essentially unstructured in nonexpressing brain cells [55,56]. This phenomenon of elevated interactions between transcriptionally active promoters and their linearly distant enhancers has been described at a plethora of loci, across many different tissues and many species, and with different 3C-derivative methods [7]. In agreement, many DNA–FISH experiments report a decrease in spatial distances between promoter and their enhancers in active tissues, for instance at the HoxD cluster

and its remote digit-specific developmental enhancers [37].

Several lines of evidence have contributed to the view that proximity not only coincidences with enhanced transcription, but it is also an essential determinant of gene expression. It was observed that engineered forced looping between enhancer and promoter coincides with increased contact frequency and leads to induced gene expression [57–61]. Forced juxtaposition between a developmentally silenced embryonic β-globin gene and the *LCR* led to its reactivation in

adult murine erythroblasts [57]. More recently, a novel light-activated dynamic looping (LADL) system that can rapidly induce distal chromatin contacts stimulated ectopic interaction between an active *Klf4* enhancer and the silent *Zfp462* gene in mouse ESCs. The novel enhancer–promoter pairing, as evidenced by 5C, coincides with an increased, modest, *Zfp462* upregulation [61].

Simultaneous live imaging of spatial and transcriptional dynamics at the *eve* locus in *Drosophila* embryo provided microscopy-based support for the importance of spatial proximity in transcriptional regulation over a large genomic distance [62]. In this experimental system, a fluorescently labeled reporter gene, which additionally allows the instantaneous measurement of transcriptional activity, was integrated 142 kb upstream of the fluorescently marked endogenous *eve* enhancer. An insulator element *homie* [63,64] was placed proximal to the reporter, self-pairing with the endogenous *homie* downstream of the enhancer, and thereby facilitating enhancer–reporter contact. Only at alleles that display high physical proximity between transgene and enhancer, a fluorescent spot of nascent transcripts was observed. When followed over time, the spatial distance between the enhancer and transgene continued to converge until a sharp increase in transcriptional activity is reached. Markedly, in the absence of the proximal *homie* and, by extension, the forced enhancer–reporter contact, the reporter gene remained nearly inactive [62]. In line with a large body of 3C-based and forced-looping studies, these findings strongly argue for the pivotal role of a spatial rendezvous of enhancer and promoter to communicate and achieve transcriptional activity.

Making space for transcription

In contrast to the aforementioned observations of increased enhancer–promoter proximity during transcription, a number of recent DNA–FISH-based and live-cell imaging studies point toward an opposite spatial behavior of *cis*-regulatory domains. Utilizing DNA–FISH, it was observed that the neural *SBE6* enhancer, at 100 kb upstream of its target gene *Shh*, spatially evades from its native promoter upon the cellular differentiation from pluripotent to neural progenitor state [65]. This increased spatial distance between enhancer and promoter is concomitant with an increase in *Shh* expression. A level of locus decompaction is also apparent upon synthetic activation of either the *Shh* promoter or the enhancer, respectively. Consistent with these findings, the dual visualization strategy Hi-M which permits simultaneous detection of

chromatin organization and nascent transcription detects a similar decondensation of local chromatin upon transcriptional activation at the *Drosophila sna* locus [4]. ORCA, an approach that is comparable to Hi-M, although detecting a weak correlation between physical distances and nascent transcripts of selected enhancer–promoter pairs, demonstrates that a number of active promoters display spatial separation from their *cis*-regulatory elements. In fact, many inactive promoters spatially reside in closer vicinity with their putative enhancers [5].

The conundrum as to whether enhancer proximity is a prerequisite for gene expression was recently addressed by another live-cell imaging study, which probes the topological behavior and transcriptional dynamics of the mammalian *Sox2* locus [66]. In mouse ESCs, the expression of the *Sox2* is fully dependent on the distal enhancer *Sox2 Control Region* (*SCR*). The *SCR* is located at ~ 100 kb downstream of the gene promoter [67,68] and, as indicated by 3C-based methods, displays highly enriched contacts with the promoter region in *Sox2*-expressing cells [28,42]. Live-cell imaging revealed that the physical distance between the *Sox2* promoter and the *SCR* varies considerably among individual cells, consistent with the cell-to-cell variations observed by the previously discussed static Oligopaint approach [5,22,23,52]. However, no association between proximity to the *SCR* and transcriptional bursting of the *Sox2* was uncovered. Interestingly, upon differentiation toward a *Sox2*-negative lineage, the locus became more spatially compacted [66]. Consistent with the above-mentioned static DNA–FISH studies, these findings argue that enhancer-mediated transcription may not be driven by an increased physical proximity between the enhancer–promoter pair. Possibly, *cis*-communication between endogenous enhancers and promoters may take place in a decompacted and accessible domain in which a further increase in proximity is not a prerequisite of transcriptional activation.

Discussion

DNA-FISH and 3C-based approaches largely agree on the existence and nature of CTs, A/B compartments, and TADs. However, they deviate in describing the finer-scale topological level, where folding is believed to directly influence long-range gene regulation. 3C-based experiments generally score enriched contacts between enhancers and promoters, in support of the concept that in order to transfer regulatory information, active enhancers must reside in close spatial proximity with their target gene. Some of the novel

microscopy measurements support this concept, but a large number appears to challenge this notion. In these studies, it is often measured that a *cis*-regulatory domain becomes rather decompacted upon activation, with physical distances between enhancer–promoter pairs increasing instead of decreasing. Strikingly, as most evident from live imaging of the *Sox2* locus, microscopy even measures increased physical distances between enhancer–promoter pairs that in 3C methods show elevated contact frequencies [66]. How is this possible?

It is essential to consider the limitations of each methodology when interpreting results produced by any assays. Proximity ligation relies on cross-linking, DNA fragmentation, and ligation, followed by NGS-based sequencing and quantification of ligation products. Reassuringly, the DNA-contact profiles produced by 3C methods are recapitulated when omitting the cross-linking step in 4C and Hi-C [69] and when interrogating the topology by ligation-free nuclear proximity assays such as split-pool recognition of interactions by tag extension [70]. Also, and importantly, DNA contacts uncovered by 4C are similarly appreciable when using an entirely independent method that relies on targeted recruitment of a DNA methyltransferase, for *in vivo* methylation measurements of chromatin interactions [71].

However, proximity ligation-dependent assays introduce biases that may hamper particularly the study of individual cells or alleles. A major limitation originates from the inherently competitive nature of proximity ligation. As a given end of a digested DNA fragment can only be ligated to one other DNA fragment, DNA fragments that share a common nuclear space and that are consequently cross-linked together compete for ligation with a given fragment's free end. In this competition, the spatially closer fragments have an advantage to fuse [7,72]. Once a given fragment ligates, it leaves the other cross-linked fragments undetected as proximal partners. Inevitably, no matter the folding of a locus, linear neighbor DNA fragments will most often be cross-linked to each other and therefore participate in competition for ligation. For single-cell or single-allele analyses, this has major implications: if a given genomic site (e.g., a promoter) through folding is brought proximal to a distant partner site (e.g., an enhancer) but ligates to its own 'boring' (noninformative) linearly proximal DNA fragment, the enhancer remains undetected as looped on this allele. 3C-based approaches are therefore most accurately referred to as 'relative proximity ligation' assays, and they rely on quantitative rather than qualitative measurement of proximal ligation events across cell populations.

Being relative, proximity ligation assays have another underappreciated consequence. As demonstrated in Fig. 2, two genomic segments (a hypothetical promoter and enhancer) in a condensed inactive chromatin fiber may be in absolute distance closer together than when looped and held together through associated large activating protein complexes in a decondensed active chromatin environment. Yet, despite being closer in space in the inactive configuration, the two may less frequently form a ligation product as intervening sequences are even closer in space, and they thus more effectively compete for ligation in the compacted fiber. Upon transcriptional activation of the locus, the decompacted surrounding chromatin may expand in space, intervening sequences become less competitive for ligation events, and hence, the looped enhancer gets relatively more proximal to the promoter, resulting in increased 3C ligation products that suggest increased contact frequencies (Fig. 2).

Providing that proximity ligation assays offer a proxy for relative contact frequencies instead of absolute or average spatial separation between genomic sites, caution should therefore be employed when modeling chromosome conformation data and when comparing them to or validating them by DNA–FISH methods. Even two decades after the first development of 3C and with upcoming approaches of ligation-free and other proximity ligation-based techniques and more advanced imaging, it remains essential to (re)consider carefully the respective methodological limitations, to eventually understand the true meaning of a 'genomic interaction'.

Acknowledgements

Conflict of interest

YH and RN declare no conflict of interest. WdL is founder and shareholder of Cergentis BV.

References

1 Giorgetti L and Heard E (2016) Closing the loop: 3C versus DNA FISH. *Genome Biol* **17** :.

2 Beliveau BJ, Joyce EF, Apostolopoulos N, Yilmaz F, Fonseka CY, McCole RB, Chang Y, Li JB, Senaratne TN, Williams BR *et al.* (2012) Versatile design and synthesis platform for visualizing genomes with Oligopaint FISH probes. *Proc Natl Acad Sci USA* **109**, 21301–21306.

Y. Huang *et al.*

Genome folding: what do DNA-FISH and proximal ligation show?

3 Fabre PJ, Benke A, Joye E, Huynh THN, Manley S and Duboule D (2015) Nanoscale spatial organization of the HoxD gene cluster in distinct transcriptional states. *Proc Natl Acad Sci USA* **112**, 13964–13969.

4 Cardozo Gizzi AM, Cattoni DI, Fiche JB, Espinola SM, Gurgo J, Messina O, Houbron C, Ogiyama Y, Papadopoulos GL, Cavalli G *et al.* (2019) Microscopy-based chromosome conformation capture enables simultaneous visualization of genome organization and transcription in intact organisms. *Mol Cell* **74**, 212–222.

5 Mateo LJ, Murphy SE, Hafner A, Cinquini IS, Walker CA and Boettiger AN (2019) Visualizing DNA folding and RNA in embryos at single-cell resolution. *Nature* **568**, 49–54.

6 Leidescher S, Nuebler J, Feodorova Y, Hildebrand E, Ullrich S, Bultmann S, Link S, Thanisch K, Dekker J, Leonhardt H *et al.* (2020) Spatial organization of transcribed eukaryotic genes. *bioRxiv.* "[PREPRINT]"

7 Denker A and De Laat W (2016) The second decade of 3C technologies: detailed insights into nuclear organization. *Genes Dev* **30**, 1357–1382.

8 Lieberman-Aiden E, Van Berkum NL, Williams L, Imakaev M, Ragoczy T, Telling A, Amit I, Lajoie BR, Sabo PJ, Dorschner MO *et al.* (2009) Comprehensive mapping of long-range interactions reveals folding principles of the human genome. *Science* **326**, 289–293.

9 Nora EP, Lajoie BR, Schulz EG, Giorgetti L, Okamoto I, Servant N, Piolot T, Van Berkum NL, Meisig J, Sedat J *et al.* (2012) Spatial partitioning of the regulatory landscape of the X-inactivation centre. *Nature* **485**, 381–385.

10 Dixon JR, Selvaraj S, Yue F, Kim A, Li Y, Shen Y, Hu M, Liu JS and Ren B (2012) Topological domains in mammalian genomes identified by analysis of chromatin interactions. *Nature* **485**, 376–380.

11 Sexton T, Yaffe E, Kenigsberg E, Bantignies F, Leblanc B, Hoichman M, Parrinello H, Tanay A and Cavalli G (2012) Three-dimensional folding and functional organization principles of the Drosophila genome. *Cell* **148**, 458–472.

12 Hsieh THS, Cattoglio C, Slobodyanyuk E, Hansen AS, Rando OJ, Tjian R and Darzacq X (2020) Resolving the 3D landscape of transcription-linked mammalian chromatin folding. *Mol Cell* **78**, 539–553.

13 Krietenstein N, Abraham S, Venev SV, Abdennur N, Gibcus J, Hsieh THS, Parsi KM, Yang L, Maehr R, Mirny LA *et al.* (2020) Ultrastructural details of mammalian chromosome architecture. *Mol Cell* **78**, 554–565.

14 Boveri TH (1909) Die Blastomerenkerne von Ascaris megalocephala und die Theorie der Chromosomenindividualität. *Arch Zellforsch* **3**, 181–268.

15 Cremer T and Cremer M (2010) Chromosome territories. *Cold Spring Harb Perspect Biol* **2**, a003889.

16 Branco MR and Pombo A (2006) Intermingling of chromosome territories in interphase suggests role in translocations and transcription-dependent associations. *PLoS Biol* **4**, e138.

17 Simonis M, Klous P, Splinter E, Moshkin Y, Willemsen R, De Wit E, Van Steensel B and De Laat W (2006) Nuclear organization of active and inactive chromatin domains uncovered by chromosome conformation capture-on-chip (4C). *Nat Genet* **38**, 1348–1354.

18 Nagano T, Lubling Y, Stevens TJ, Schoenfelder S, Yaffe E, Dean W, Laue ED, Tanay A and Fraser P (2013) Single-cell Hi-C reveals cell-to-cell variability in chromosome structure. *Nature* **502**, 59–64.

19 Selvaraj S, Dixon JR, Bansal V and Ren B (2013) Whole-genome haplotype reconstruction using proximity-ligation and shotgun sequencing. *Nat Biotechnol* **31**, 1111–1118.

20 Osborne CS, Chakalova L, Brown KE, Carter D, Horton A, Debrand E, Goyenechea B, Mitchell JA, Lopes S, Reik W *et al.* (2004) Active genes dynamically colocalize to shared sites of ongoing transcription. *Nat Genet* **36**, 1065–1071.

21 Rao SSP, Huntley MH, Durand NC, Stamenova EK, Bochkov ID, Robinson JT, Sanborn AL, Machol I, Omer AD, Lander ES *et al.* (2014) A 3D map of the human genome at kilobase resolution reveals principles of chromatin looping. *Cell* **159**, 1665–1680.

22 Wang S, Su JH, Beliveau BJ, Bintu B, Moffitt JR, Wu CT and Zhuang X (2016) Spatial organization of chromatin domains and compartments in single chromosomes. *Science* **353**, 598–602.

23 Bintu B, Mateo LJ, Su JH, Sinnott-Armstrong NA, Parker M, Kinrot S, Yamaya K, Boettiger AN and Zhuang X (2018) Super-resolution chromatin tracing reveals domains and cooperative interactions in single cells. *Science* **362**, eaau1783.

24 Bertero A, Fields PA, Ramani V, Bonora G, Yardimci GG, Reinecke H, Pabon L, Noble WS, Shendure J and Murry CE (2019) Dynamics of genome reorganization during human cardiogenesis reveal an RBM20-dependent splicing factory. *Nat Commun* **10**, 1538.

25 Dixon JR, Jung I, Selvaraj S, Shen Y, Antosiewicz-Bourget JE, Lee AY, Ye Z, Kim A, Rajagopal N, Xie W *et al.* (2015) Chromatin architecture reorganization during stem cell differentiation. *Nature* **518**, 331–336.

26 Vilarrasa-Blasi R, Soler-Vila P, Verdaguer-Dot N, Russiñol N, Di Stefano M, Chapaprieta V, Clot G, Farabella I, Cuscó P, Agirre X *et al.* (2019) Dynamics of genome architecture and chromatin function during human B cell differentiation and neoplastic transformation. *bioRxiv.* [PREPRINT]

27 Nothjunge S, Nührenberg TG, Grüning BA, Doppler SA, Preissl S, Schwaderer M, Rommel C, Krane M, Hein L and Gilsbach R (2017) DNA methylation

signatures follow preformed chromatin compartments in cardiac myocytes. *Nat Commun* 8, 1667.

28 Bonev B, Mendelson Cohen N, Szabo Q, Fritsch L, Papadopoulos GL, Lubling Y, Xu X, Lv X, Hugnot JP, Tanay A *et al.* (2017) Multiscale 3D genome rewiring during mouse neural development. *Cell* 171, 557–572.

29 Krijger PHL, Di Stefano B, De Wit E, Limone F, Van Oevelen C, De Laat W and Graf T (2016) Cell-of-origin-specific 3D genome structure acquired during somatic cell reprogramming. *Cell Stem Cell* 18, 597–610.

30 Wijchers PJ, Krijger PHL, Geeven G, Zhu Y, Denker A, Verstegen MJAM, Valdes-Quezada C, Vermeulen C, Janssen M, Teunissen H *et al.* (2016) Cause and consequence of tethering a SubTAD to different nuclear compartments. *Mol Cell* 61, 461–473.

31 Lin YC, Benner C, Mansson R, Heinz S, Miyazaki K, Miyazaki M, Chandra V, Bossen C, Glass CK and Murre C (2012) Global changes in the nuclear positioning of genes and intra-and interdomain genomic interactions that orchestrate B cell fate. *Nat Immunol* 13, 1196–1204.

32 Kind J, Pagie L, De Vries SS, Nahidiazar L, Dey SS, Bienko M, Zhan Y, Lajoie B, De Graaf CA, Amendola M *et al.* (2015) Genome-wide maps of nuclear lamina interactions in single human cells. *Cell* 163, 134–147.

33 Girelli G, Custodio J, Kallas T, Agostini F, Wernersson E, Spanjaard B, Mota A, Kolbeinsdottir S, Gelali E, Crosetto N *et al.* (2020) GPSeq reveals the radial organization of chromatin in the cell nucleus. *Nat Biotechnol* 38, 1184–1193.

34 Lupiáñez DG, Kraft K, Heinrich V, Krawitz P, Brancati F, Klopocki E, Horn D, Kayserili H, Opitz JM, Laxova R *et al.* (2015) Disruptions of topological chromatin domains cause pathogenic rewiring of gene-enhancer interactions. *Cell* 161, 1012–1025.

35 Franke M, Ibrahim DM, Andrey G, Schwarzer W, Heinrich V, Schöpflin R, Kraft K, Kempfer R, Jerković I, Chan WL *et al.* (2016) Formation of new chromatin domains determines pathogenicity of genomic duplications. *Nature* 538, 265–269.

36 Symmons O, Pan L, Remeseiro S, Aktas T, Klein F, Huber W and Spitz F (2016) The Shh topological domain facilitates the action of remote enhancers by reducing the effects of genomic distances. *Dev Cell* 39, 529–543.

37 Fabre PJ, Leleu M, Mormann BH, Lopez-Delisle L, Noordermeer D, Beccari L and Duboule D (2017) Large scale genomic reorganization of topological domains at the HoxD locus. *Genome Biol* 18, 149.

38 Remeseiro S, Hörnblad A and Spitz F (2016) Gene regulation during development in the light of topologically associating domains. *Wiley Interdiscip Rev Dev Biol* 5, 169–185.

39 Nasmyth K (2001) Disseminating the genome: joining, resolving, and separating sister chromatids during mitosis and meiosis. *Annu Rev Genet* 35, 673–745.

40 Alipour E and Marko JF (2012) Self-organization of domain structures by DNA-loop-extruding enzymes. *Nucleic Acids Res* 40, 11202–11212.

41 Fudenberg G, Imakaev M, Lu C, Goloborodko A, Abdennur N and Mirny LA (2016) Formation of chromosomal domains by loop extrusion. *Cell Rep* 15, 2038–2049.

42 de Wit E, Vos ESM, Holwerda SJB, Valdes-Quezada C, Verstegen MJAM, Teunissen H, Splinter E, Wijchers PJ, Krijger PHL and de Laat W (2015) CTCF binding polarity determines chromatin looping. *Mol Cell* 60, 676–684.

43 Guo Y, Xu Q, Canzio D, Shou J, Li J, Gorkin DU, Jung I, Wu H, Zhai Y, Tang Y *et al.* (2015) CRISPR inversion of CTCF sites alters genome topology and enhancer/promoter function. *Cell* 162, 900–910.

44 Sanborn AL, Rao SSP, Huang SC, Durand NC, Huntley MH, Jewett AI, Bochkov ID, Chinnappan D, Cutkosky A, Li J *et al.* (2015) Chromatin extrusion explains key features of loop and domain formation in wild-type and engineered genomes. *Proc Natl Acad Sci USA* 112, E6456–E6465.

45 Nora EP, Goloborodko A, Valton AL, Gibcus JH, Uebersohn A, Abdennur N, Dekker J, Mirny LA and Bruneau BG (2017) Targeted degradation of CTCF decouples local insulation of chromosome domains from genomic compartmentalization. *Cell* 169, 930–944.

46 Schwarzer W, Abdennur N, Goloborodko A, Pekowska A, Fudenberg G, Loe-Mie Y, Fonseca NA, Huber W, Haering CH, Mirny L *et al.* (2017) Two independent modes of chromatin organization revealed by cohesin removal. *Nature* 551, 51–56.

47 Rao SSP, Huang SC, Glenn St Hilaire B, Engreitz JM, Perez EM, Kieffer-Kwon KR, Sanborn AL, Johnstone SE, Bascom GD, Bochkov ID *et al.* (2017) Cohesin loss eliminates all loop domains. *Cell* 171, 305–320.

48 Zhang H, Emerson DJ, Gilgenast TG, Titus KR, Lan Y, Huang P, Zhang D, Wang H, Keller CA, Giardine B *et al.* (2019) Chromatin structure dynamics during the mitosis-to-G1 phase transition. *Nature* 576, 158–162.

49 Nagano T, Lubling Y, Várnai C, Dudley C, Leung W, Baran Y, Mendelson Cohen N, Wingett S, Fraser P and Tanay A (2017) Cell-cycle dynamics of chromosomal organization at single-cell resolution. *Nature* 547, 61–67.

50 Stevens TJ, Lando D, Basu S, Atkinson LP, Cao Y, Lee SF, Leeb M, Wohlfahrt KJ, Boucher W, O'Shaughnessy-Kirwan A *et al.* (2017) 3D structures of individual mammalian genomes studied by single-cell Hi-C. *Nature* 544, 59–64.

Y. Huang *et al.*

Genome folding: what do DNA-FISH and proximal ligation show?

51 Finn EH, Pegoraro G, Brandão HB, Valton AL, Oomen ME, Dekker J, Mirny L and Misteli T (2019) Extensive heterogeneity and intrinsic variation in spatial genome organization. *Cell* **176**, 1502–1515.

52 Szabo Q, Jost D, Chang JM, Cattoni DI, Papadopoulos GL, Bonev B, Sexton T, Gurgo J, Jacquier C, Nollmann M *et al.* (2018) TADs are 3D structural units of higher-order chromosome organization in Drosophila. *Sci Adv* **4**, eaar8082.

53 Luppino JM, Park DS, Nguyen SC, Lan Y, Xu Z, Yunker R and Joyce EF (2020) Cohesin promotes stochastic domain intermingling to ensure proper regulation of boundary-proximal genes. *Nat Genet* **52**, 840–848.

54 de Wit E (2020) TADs as the caller calls them. *J Mol Biol.* **432**, 638–642.

55 Tolhuis B, Palstra RJ, Splinter E, Grosveld F and De Laat W (2002) Looping and interaction between hypersensitive sites in the active β-globin locus. *Mol Cell* **10**, 1453–1465.

56 Van De Werken HJG, Landan G, Holwerda SJB, Hoichman M, Klous P, Chachik R, Splinter E, Valdes-Quezada C, Öz Y, Bouwman BAM *et al.* (2012) Robust 4C-seq data analysis to screen for regulatory DNA interactions. *Nat Methods* **9**, 969–972.

57 Deng W, Rupon JW, Krivega I, Breda L, Motta I, Jahn KS, Reik A, Gregory PD, Rivella S, Dean A *et al.* (2014) Reactivation of developmentally silenced globin genes by forced chromatin looping. *Cell* **158**, 849–860.

58 Deng W, Lee J, Wang H, Miller J, Reik A, Gregory PD, Dean A and Blobel GA (2012) Controlling long-range genomic interactions at a native locus by targeted tethering of a looping factor. *Cell* **149**, 1233–1244.

59 Morgan SL, Mariano NC, Bermudez A, Arruda NL, Wu F, Luo Y, Shankar G, Jia L, Chen H, Hu JF *et al.* (2017) Manipulation of nuclear architecture through CRISPR-mediated chromosomal looping. *Nat Commun* **8**, 15993.

60 Hao N, Shearwin KE and Dodd IB (2017) Programmable DNA looping using engineered bivalent dCas9 complexes. *Nat Commun* **8**, 1628.

61 Kim JH, Rege M, Valeri J, Dunagin MC, Metzger A, Titus KR, Gilgenast TG, Gong W, Beagan JA, Raj A *et al.* (2019) LADL: light-activated dynamic looping for endogenous gene expression control. *Nat Methods* **16**, 633–639.

62 Chen H, Levo M, Barinov L, Fujioka M, Jaynes JB and Gregor T (2018) Dynamic interplay between enhancer–promoter topology and gene activity. *Nat Genet* **50**, 1296–1303.

63 Fujioka M, Wu X and Jaynes JB (2009) A chromatin insulator mediates transgene homing and very long-range enhancer-promoter communication. *Development* **136**, 3077–3087.

64 Fujioka M, Sun G and Jaynes JB (2013) The Drosophila eve insulator homie promotes eve expression and protects the adjacent gene from repression by polycomb spreading. *PLoS Genet* **9**, e1003883.

65 Benabdallah NS, Williamson I, Illingworth RS, Kane L, Boyle S, Sengupta D, Grimes GR, Therizols P and Bickmore WA (2019) Decreased enhancer-promoter proximity accompanying enhancer activation. *Mol Cell* **76**, 473–484.

66 Alexander JM, Guan J, Li B, Maliskova L, Song M, Shen Y, Huang B, Lomvardas S and Weiner OD (2019) Live-cell imaging reveals enhancer-dependent sox2 transcription in the absence of enhancer proximity. *Elife* **8**, e41769.

67 Li Y, Rivera CM, Ishii H, Jin F, Selvaraj S, Lee AY, Dixon JR and Ren B (2014) CRISPR reveals a distal super-enhancer required for Sox2 expression in mouse embryonic stem cells. *PLoS One* **9**, e114485.

68 Zhou HY, Katsman Y, Dhaliwal NK, Davidson S, Macpherson NN, Sakthidevi M, Collura F and Mitchell JA (2014) A Sox2 distal enhancer cluster regulates embryonic stem cell differentiation potential. *Genes Dev* **28**, 2699–2711.

69 Brant L, Georgomanolis T, Nikolic M, Brackley CA, Kolovos P, Ijcken W, Grosveld FG, Marenduzzo D and Papantonis A (2016) Exploiting native forces to capture chromosome conformation in mammalian cell nuclei. *Mol Syst Biol* **12**, 891.

70 Quinodoz SA, Ollikainen N, Tabak B, Palla A, Schmidt JM, Detmar E, Lai MM, Shishkin AA, Bhat P, Takei Y *et al.* (2018) Higher-order inter-chromosomal hubs shape 3D genome organization in the nucleus. *Cell* **174**, 744–757.

71 Redolfi J, Zhan Y, Valdes-Quezada C, Kryzhanovska M, Guerreiro I, Iesmantavicius V, Pollex T, Grand RS, Mulugeta E, Kind J *et al.* (2019) DamC reveals principles of chromatin folding *in vivo* without crosslinking and ligation. *Nat Struct Mol Biol* **26**, 471–480.

72 de Wit E and de Laat W (2012) A decade of 3C technologies: Insights into nuclear organization. *Genes Dev* **26**, 11–24.